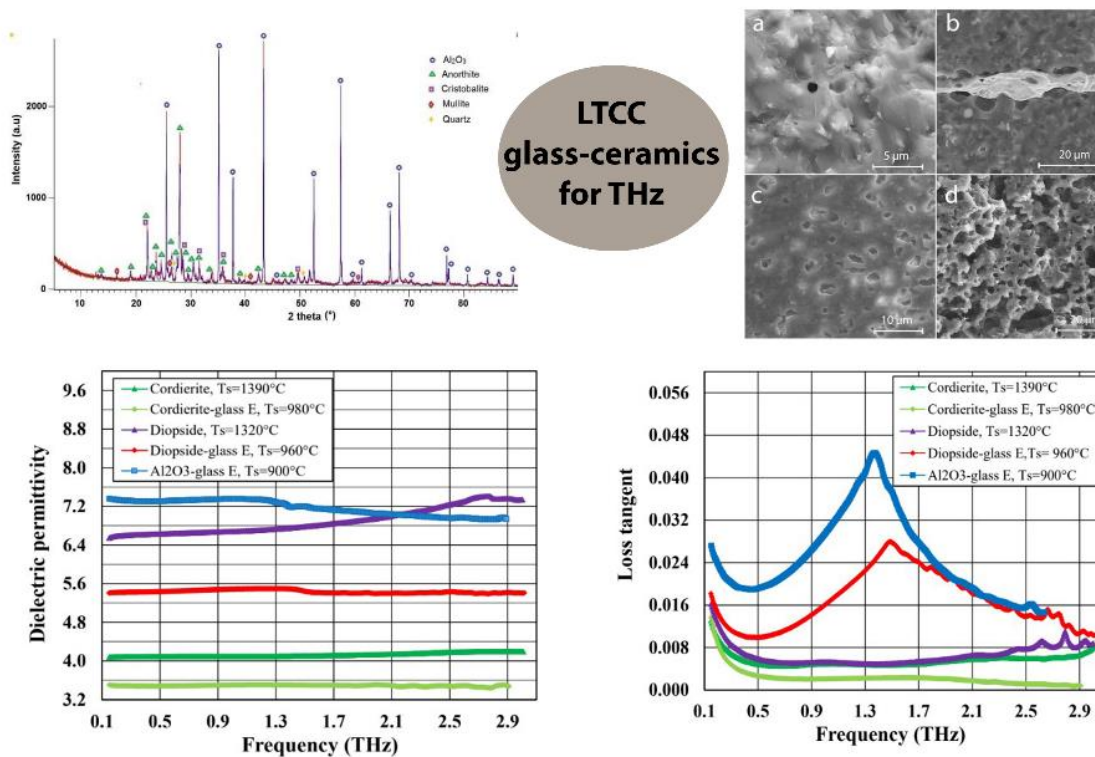


LTCC glass-ceramics based on diopside/cordierite/ Al_2O_3 for ultra-high frequency applications

Beata Synkiewicz-Musialska⁽¹⁾ ✉

⁽¹⁾Łukasiewicz Research Network - Institute of Microelectronics and Photonics, ul. Zabłocie 39, 30-701 Kraków

✉ Correspondence to: beata.synkiewicz.musialska@imif.lukasiewicz.gov.pl



Abstract: In this work, three glass-ceramic composites based on a commercial $\text{SiO}_2\text{-B}_2\text{O}_3\text{-Al}_2\text{O}_3\text{-CaO-MgO}$ glass and cordierite, diopside or Al_2O_3 were used for preparation of green tapes and low temperature cofired ceramics (LTCC) substrates. The thermal behavior, phase composition, microstructure and dielectric properties of the fabricated glass-ceramics were characterized using a heating microscope, thermal analysis, X-ray diffraction, scanning electron microscopy and time domain spectroscopy. The applicability of the

developed materials for LTCC technology was demonstrated by the preparation of test multilayer substrates. The glass-ceramic substrates exhibit advantageous properties for ultra-high frequency LTCC applications, including low sintering temperatures of 900-980°C, good compatibility with commercial Ag and AgPd conductive pastes and a low dielectric permittivity of 3.5-7 at 1 THz.

Keywords: glass ceramics, diopside, cordierite, Al₂O₃, LTCC technology, THz dielectric properties

Received: 2023.04.18

Accepted: 2023.06.18

Published: 2023.06.26

DOI: 10.58332/scirad2023v2i2a04

Introduction

Low temperature cofired ceramics (LTCC) technology is a relatively inexpensive and simple method which enables manufacturing multilayer electronic modules of high miniaturization degree, integration scale and reliability. The conventional LTCC process embraces tape casting of green ceramic tapes, cutting of vias for electrical connections between layers, filling of vias and deposition of thick film conductors and resistors on green sheets by screen printing, stacking of green sheets, isostatic lamination and cofiring of ceramic tapes with thick films. The typical sintering temperature of LTCC materials is below 950-1000°C to enable cofiring with thick film conductors made of cheap commercial silver and silver-palladium pastes. One of the important applications of LTCC technology are complex substrates and packages for high frequency electronic devices. Dynamic development of 5th and 6th generation (5G and 6G) wireless communication systems shifts their operating frequency from GHz range (microwaves) to THz range (submillimeter waves). The materials appropriate for the substrates of very high frequency systems should meet some specific requirements. These are low dielectric permittivity, low dielectric loss and temperature stability of dielectric permittivity. Low dielectric permittivity is advantageous for reducing signal propagation delay, crosstalk between signal lines and electronic device size, low dielectric loss decreases power consumption and improves frequency selectivity, while low temperature coefficient of dielectric permittivity enables avoiding the influence of temperature fluctuations on operating frequency.

Among the materials with a low intrinsic dielectric permittivity are ceramics, glasses and glass-ceramics rich in SiO₂ and/or B₂O₃ [1-4], silicates, like cordierite Mg₂Al₄Si₅O₁₈ [5-13], diopside CaMgSi₂O₆ [14-17], willemite Zn₂SiO₄ [18,19], forsterite Mg₂SiO₄ [20], some borates, tungstates, phosphates, molybdates. Majority of the polycrystalline ceramic materials are not directly applicable in LTCC technology due to too high sintering

temperatures. Thus, the popular solution is combining the polycrystalline ceramics with low melting glasses. Typical LTCC dielectric materials were classified by Zhou [21] into three groups: glass-ceramics, glass ceramic composites, and glass bonded ceramics. The first group includes materials in which the glass undergoes intensive crystallization, but the glass content remains high (50-80%). For the most widely used second group, the starting materials form a mixture of glass and ceramics with a glass content of 20-50%. For the third group, about 10% glass is added to the ceramics to act as a sintering aid.

Luo *et al.* [4] investigated the properties of borosilicate glass/ Al_2O_3 composites with different Al_2O_3 concentrations for LTCC applications. The LTCC composites were composed of the α - Al_2O_3 phase, anorthite phase ($\text{CaO}\cdot\text{Al}_2\text{O}_3\cdot 2\text{SiO}_2$), cristobalite phase (SiO_2) and amorphous glass phase. The substrates showed a dielectric permittivity of 8.08 and a dielectric loss of 0.9×10^{-3} at 7 GHz.

Lou *et al.* [5] investigated phase structure, microstructure, and microwave dielectric properties of $\text{Mg}_{1.8}\text{R}_{0.2}\text{Al}_4\text{Si}_5\text{O}_{18}$ (R = Mg, Ca, Sr, Ba, Mn, Co, Ni, Cu, Zn) cordierite ceramics. The optimal microwave dielectric properties were obtained for $\text{Mg}_{1.8}\text{Ni}_{0.2}\text{Al}_4\text{Si}_5\text{O}_{18}$ – dielectric permittivity of 4.53, quality factor $Q \times f$ of 61880 GHz and temperature coefficient of resonant frequency of -32 ppm/°C. A 5G-Sub 6 GHz patch antenna with a central frequency of 4.91 GHz, a gain of 5.83 dBi and an efficiency of 76 % was successfully designed and fabricated using a $\text{Mg}_{1.8}\text{Ni}_{0.2}\text{Al}_4\text{Si}_5\text{O}_{18}$ substrate [5].

Ohsato *et al.* [6] fabricated indialite/cordierite glass-ceramics with the addition of 10 wt.% TiO_2 or 10 wt.% Bi_2O_3 . These materials exhibit excellent microwave dielectric properties – a low dielectric permittivity of 5.6-6.1 and a high quality factor of 80000-120000 GHz. The glass-ceramics were applied to dielectric resonators and low-temperature co-fired ceramic (LTCC) substrates for 5G/6G mobile communication systems.

Seeking new materials which preserve good dielectric properties at ultra-high terahertz frequencies is an important goal of this work. In literature, there are very few reports on dielectric properties of substrate materials in terahertz range. In this work, the glass-ceramic composites based on diopside, cordierite or Al_2O_3 mixed with a commercial SiO_2 - B_2O_3 - Al_2O_3 - CaO - MgO glass E were applied as materials for LTCC substrates and their dielectric parameters in the terahertz range were presented for the first time. In our previous publications, we report the THz dielectric characteristics of several other ceramic and glass-ceramic LTCC materials [3,19].

Results and discussion

Figure 1 presents selected images from a heating microscope for glass E, diopside-glass, cordierite-glass and Al₂O₃-glass samples. For glass E, softening temperature is 870°C, melting point corresponding to the hemisphere formation was observed at 1076°C and reflow takes place at 1216°C (Fig.1a). The start of shrinking occurs at about 830, 920 and 800°C, while the optimal sintering temperatures were found to be about 960, 980 and 900°C for diopside-glass, cordierite-glass and Al₂O₃-glass composites, respectively (Fig.1b,c,d). At higher temperatures, a distinct effect of increase of sample sizes was observed for diopside-glass, probably due to glass crystallization effect. Melting points were about 1240°C for diopside-glass, 1235°C for cordierite-glass and above 1300°C for Al₂O₃-glass composites, respectively.

Figure 2a illustrates the temperature and mass changes during heating of a diopside-glass sample, determined by differential thermal analysis (DTA) and thermogravimetric (TG, DTG) studies. Both the TG and the DTA curves have flat courses, which implies that the composition and structure of the composite remain stable in the investigated temperature range. A slight weight loss (2.6%) is observed up to 660°C. The weight loss at lower temperatures and the corresponding small endothermic peak at about 92°C are associated with evaporation of water absorbed in the sample. A slight increase in sample temperature occurs up to 790°C. No strong thermal effects related to phase transitions, redox reactions, crystallization were observed. A small peak at 787°C was attributed to the crystallization of glass E. The local minimum in the DTA curve at 965°C corresponds to the glass E softening.

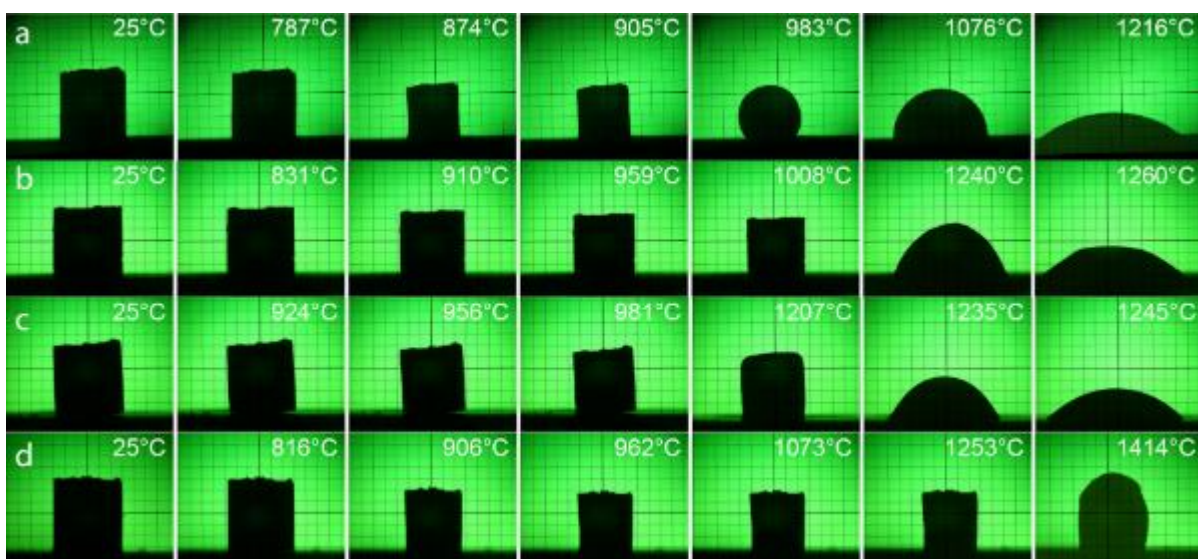
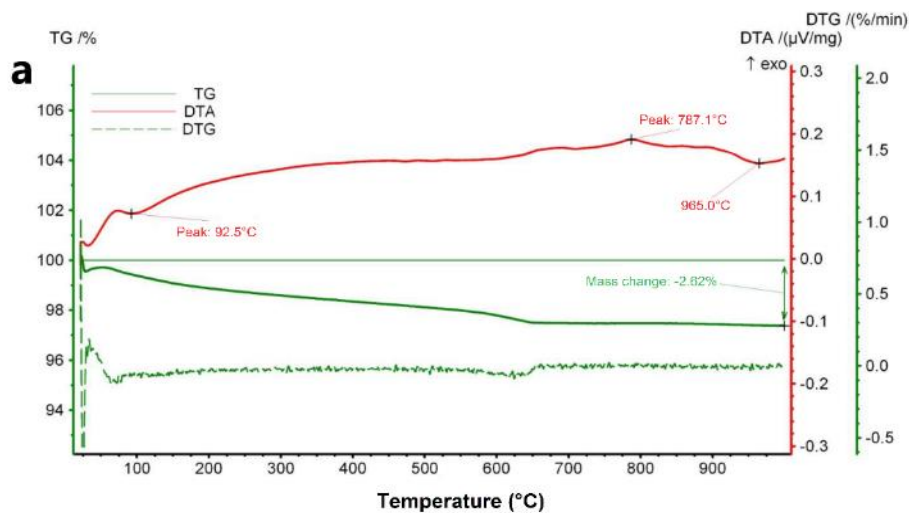


Fig. 1. Selected images from a heating microscope for (a) glass E, (b) diopside-glass E, (c) cordierite-glass E, (d) Al₂O₃-glass E in the temperature range 20-1270°C.

For diopside-glass, the XRD analysis (Fig.2b) reveals the presence of additional phases crystallizing from glass E - cristobalite, wollastonite CaSiO_3 and anortite $\text{CaAl}_2\text{Si}_2\text{O}_8$.

For Al_2O_3 -glass, the XRD analysis shows a significant amount of an additional crystalline phase, anorthite, that crystallizes from glass E, as well as the presence of small amounts of cristobalite, quartz and mullite (Fig.3). Figure 4a presents the image from an optical microscope of a test pattern of conductive paths made of commercial AgPd paste screen printed on a green tape based on diopside-glass. Figure 4b shows the test pattern after cofiring with LTCC substrate.

SEM images in Figures 5a and 5b reveal high densification of Al_2O_3 -glass layer in the LTCC substrate and its low closed porosity. Based on SEM observations (Fig.5b), no delaminations, cracks, secondary phases or excessive pore formation were found at the interface between Ag based thick film internal electrodes and ceramic layers. This implies good compatibility of the commercial conductor thick film paste with the developed glass-ceramic composite. Figures 5c and 5d show diopside-glass and cordierite-glass LTCC substrates, respectively. These materials are characterized by the presence of a significant, evenly distributed closed porosity. The reason for this effect could be too high viscosity of the glass to enable filling the pores by viscous flow and a decreased glass sintering rate due to its crystallization.



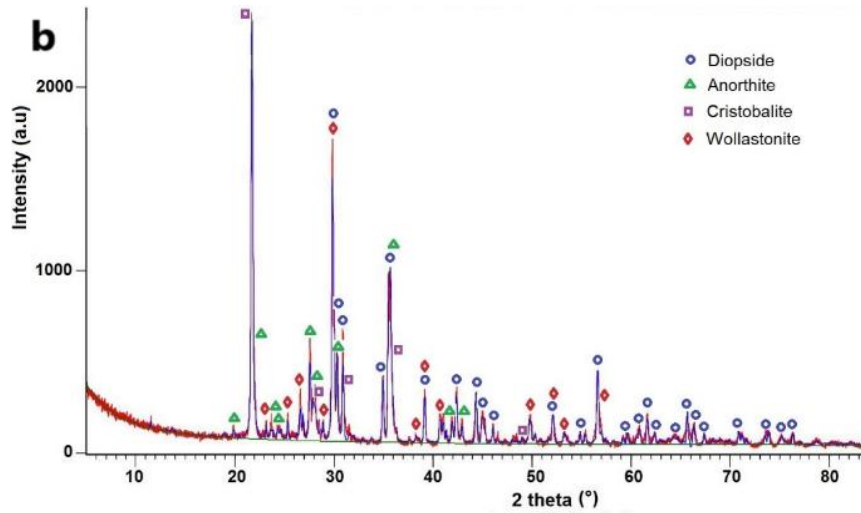


Fig. 2. (a) The results of thermal analysis (TG-DTG-DTA curves) and (b) diffraction pattern for diopside-glass composite.

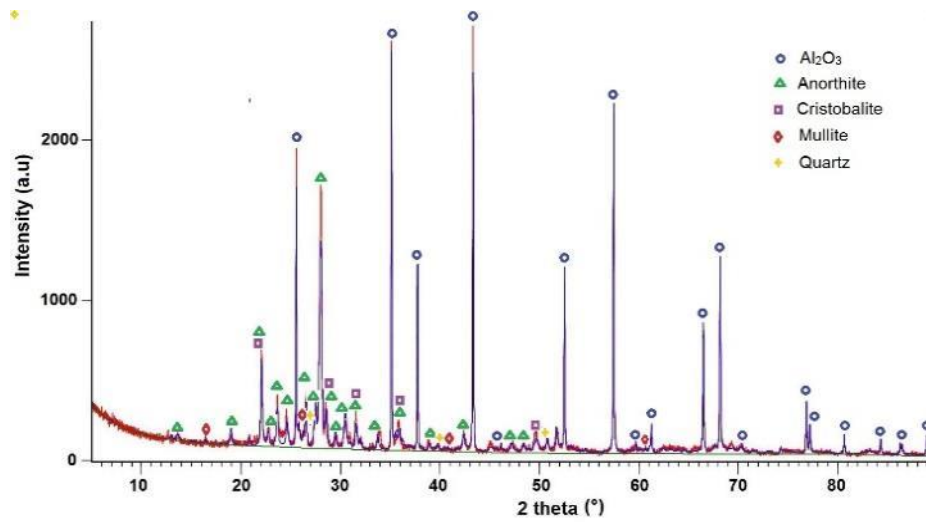


Fig. 3. Diffraction pattern for Al₂O₃-glass composite.

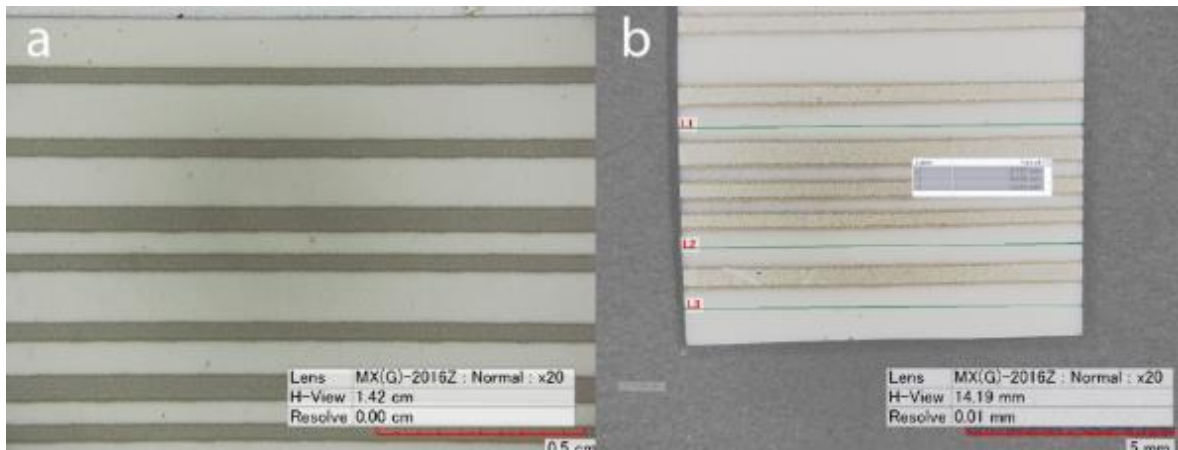


Fig. 4. Images from a digital optical microscope of test conductor pattern made of commercial AgPd paste: (a) screen printed on green tape, (b) cofired with LTCC substrate based on diopside-glass.

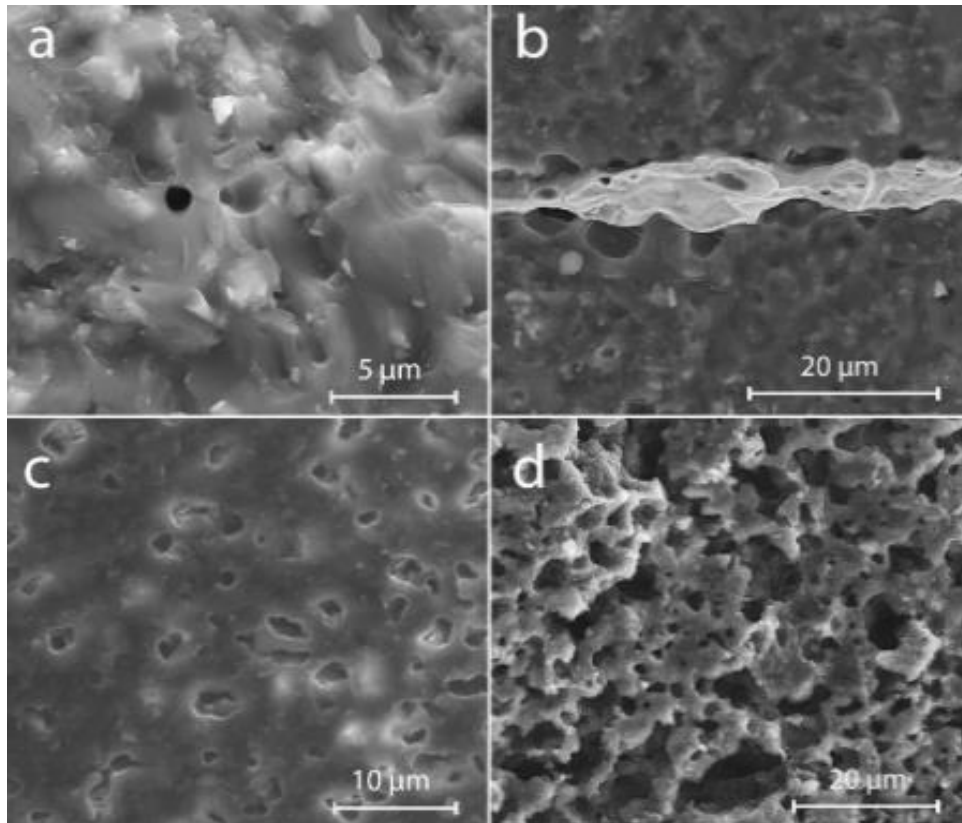


Fig. 5. SEM images of fractured cross-section of glass-ceramic layers in LTCC structures: (a) Al₂O₃-glass E, (b) the interface between Al₂O₃-glass E and AgPd thick film internal electrodes, (c) diopside-glass E, (d) cordierite-glass E.

Figures 6a and 6b depict the dielectric permittivity and loss tangent versus frequency in the 0.1-3 THz range for diopside-glass, cordierite-glass and Al₂O₃-glass substrates, sintered at 960, 980 and 900°C, respectively. For comparison, the characteristics for diopside and cordierite substrates sintered at much higher temperatures (1320 and 1390°C) are also presented. The shape of the frequency dependences is similar for all materials in the lower frequency range. The dielectric permittivity exhibits slight changes in the range 0.15-1.3 THz. At 1 THz, dielectric permittivities are 5.5, 3.5 and 7.4 for diopside-glass, cordierite-glass and Al₂O₃-glass, respectively.

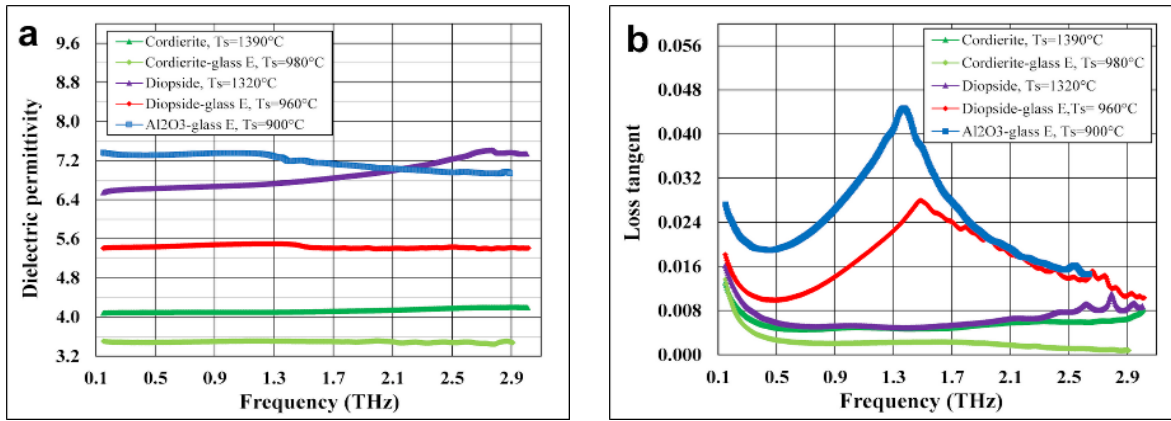


Fig. 6. Comparison of the frequency dependences of dielectric permittivity (a) and loss tangent (b) in the 0.1-3 THz range for diopside-glass E, cordierite-glass, Al₂O₃-glass E, diopside and cordierite substrates

The lowest dielectric permittivity (3.5 at 1 THz) was attained for cordierite-glass substrates. The loss tangent shows the minimum values of 0.009, 0.002 and 0.019 in the 0.5-0.7 THz range for diopside-glass, cordierite-glass and Al₂O₃-glass, respectively. For pure cordierite, both the dielectric permittivity and the loss tangent are low and slightly changing with frequency (4.1 and <0.005 in the 0.4-1.8 THz range, respectively). Diopside ceramics shows a higher dielectric permittivity of 6.7 and a relatively low loss tangent of 0.005 at 1 THz. Apart from pure cordierite and Al₂O₃-glass, low dielectric permittivity of these materials is related to a significant contribution of closed porosity (6-12%).

For the tested glass-ceramics, the dielectric loss is generally much higher, and the frequency dependence of the loss tangent exhibits a broad maximum above 1 THz for diopside-glass and cordierite-glass. The reason for the increased loss of glass-ceramics compared to polycrystalline materials is multiphase composition, great amount of glassy phase and significant fraction of pores on which phonon scattering can occur.

The dielectric properties of the materials fabricated in this work were close to those reported by other authors for similar type glass-ceramic composites [3-6,9-12,14]. However, in contrast to the majority of previous studies, the dielectric properties in this work were characterized at much higher frequencies (in the THz range, not in the GHz range) and feasibility of substrates based on the developed materials in LTCC technology was proved experimentally. Furthermore, the performed studies enabled comparing the compatibility of the commercial glass E, with three kinds of conventional ceramics – alumina, diopside and cordierite. The dielectric properties of the developed materials were also close to those of commercial LTCC tapes offered by DuPont (dielectric permittivity of 7.61 and dielectric loss of 0.097 at 1 THz for 951 tape) and Ferro (dielectric permittivity of 6.06 and dielectric loss of 0.012 at 1 THz for A6M tape) [22].

Materials and methods

In this work, the commercial glass E and alternatively cordierite $Mg_2Al_4Si_5O_{18}$, diopside $CaMgSi_2O_6$ or Al_2O_3 were used as the polycrystalline components of the slurries for ceramic tapes casting. Glass E was produced in the "Szczakowa" glassworks (Poland). The glass composition is 54.1wt% SiO_2 , 8.5wt% B_2O_3 , 14.5wt% Al_2O_3 , 20.5wt% CaO and 1.5wt.% MgO . This glass was destined for electronic applications, has a low content of alkaline elements to ensure high resistivity, and exhibits the crystallization tendency which is advantageous for improving mechanical and thermal properties of the material after thermal treatment.

Cordierite and diopside are very good candidates for high frequency substrates due to their low dielectric permittivity of about 4.5 and 7.6, respectively. Alumina Al_2O_3 is the most popular substrate material in thick film technology with the perfect compatibility with majority of commercial conductive pastes. Its dielectric permittivity of about 9.8 at 1 GHz is relatively high.

Cordierite and diopside were synthesized from the reagent grade starting materials MgO , Al_2O_3 and SiO_2 (99.9%, Sigma Aldrich, Germany) by solid state reaction method at 1350 and 1300°C, respectively. The syntheses products were ball milled (Fritsch, Germany) for 8 h. Glass and ceramic powders, mixed in 1:1 weight ratio, were ball milled with organic additives in order to obtain slurries for tape casting. As organic additives were used: polyvinyl butyral as a binder, fish oil as dispersant, dibutyl phthalate and polyethylene glycol as plasticizers, toluene and isopropyl alcohol as solvents. LTCC substrates were prepared by tape casting (R.Mistler, USA), laser cutting (Oxford Lasers, UK), stacking, isostatic pressing (Pacific Trinetics Corporation, USA), screen printing of conductive layers (Microtec, Japan) and cofiring at 900-980°C.

The phase composition was examined by XRD method (Empyrean, PANalytical, Netherlands). Based on the observation in a heating microscope (Leitz, Germany) the characteristic temperatures of the start of shrinking, optimal sintering, softening and melting were determined for the samples during heating up to 1300°C. Thermal effects and mass changes in the temperature range 20-1000°C were determined using differential thermal analysis (DTA), thermogravimetric (TG) and differential thermogravimetric (DTG) studies (Netzsch, Germany). The microstructure of the ceramics and cooperation with conductive thick films was investigated in scanning electron microscope (FEI, USA) and digital optical microscope (Hirox, Japan). Dielectric properties were studied in the 0.15-3 THz range using

time domain spectroscopy (TDS) method (Teraview, UK) [19] in cooperation with Military University of Technology in Warsaw.

Conclusions

Applicability of a commercial glass E for fabrication of low dielectric permittivity substrates which are feasible using LTCC technology was confirmed based on thermal, microstructural and dielectric properties studies. For three investigated compositions of glass-ceramic composites containing cordierite, diopside or alumina as polycrystalline components, the planned effect of lowering of the sintering temperature to a level below 1000°C was attained and commercial Ag and AgPd thick film conductive pastes were successfully applied in the test LTCC structures. The glass-ceramic substrates based on glass E and diopside/cordierite/ Al_2O_3 exhibited advantageous low dielectric permittivities of 3.5-7 at 1 THz. The microstructure of the fabricated substrates based on alumina-glass was dense, while for diopside-glass and cordierite-glass contained closed porosity which contributed to lowering of the dielectric permittivity.

Acknowledgements

The work has been financed by the National Science Centre, Poland, grant number 2019/35/B/ST5/02674.

References

- [1] Hu, C.; Liu, P.; Microwave dielectric properties of SiO_2 ceramics with addition of Li_2TiO_3 . *Mater. Res. Bull.* **2015**, 65, 132-136. DOI: [10.1016/j.materresbull.2015.01.034](https://doi.org/10.1016/j.materresbull.2015.01.034)
- [2] Li, L.; Liu, C.H.; Zhu, J.Y.; Chen, X.M.; B_2O_3 -modified fused silica microwave dielectric materials with ultra-low dielectric constant. *J. Eur. Ceram. Soc.* **2015**, 35, 1799-1805. DOI: [10.1016/j.jeurceramsoc.2014.12.016](https://doi.org/10.1016/j.jeurceramsoc.2014.12.016)
- [3] Synkiewicz-Musialska, B.; Szwagierczak, D.; Kulawik, J.; Pałka, N.; Piasecki, P.; Structural, thermal and dielectric properties of low dielectric permittivity cordierite-mullite-glass substrates at terahertz frequencies. *Materials* **2021**, 14, 4030. DOI: [10.3390/ma14144030](https://doi.org/10.3390/ma14144030)
- [4] Luo, X.; Tao, H.; Li, P.; Fu, Y.; Zhou, H.; Properties of borosilicate glass/ Al_2O_3 composites with different Al_2O_3 concentrations for LTCC applications. *J. Mater. Sci.: Mater. Electron.* **2020**, 31, 14069-14077. DOI: [10.1007/s10854-020-03961-z](https://doi.org/10.1007/s10854-020-03961-z)
- [5] Lou, W.; Song, K.; Hussain, F.; Khesro, A.; Zhao, J.; Bafrooei, H.B.; Zhou, T.; Liu, B.; Mao, M.; Xu, K.; Taheri-nassaj, E.; Zhou, D.; Luo, S.; Sun, S.; Lin, H.; Wang, D.;

- Microwave dielectric properties of $\text{Mg}_{1.8}\text{R}_{0.2}\text{Al}_4\text{Si}_5\text{O}_{18}$ (R = Mg, Ca, Sr, Ba, Mn, Co, Ni, Cu, Zn) cordierite ceramics and their application for 5G microstrip patch antenna. *J. Eur. Ceram. Soc.* **2022**, 42, 2254-2260. DOI: [10.1016/j.jeurceramsoc.2021.12.050](https://doi.org/10.1016/j.jeurceramsoc.2021.12.050)
- [6] Ohsato, H.; Varghese, J.; Kan, A.; Kim, J.S.; Kagomiya, I.; Ogawa, H.; Sebastian, M.T.; Jantunen, H.; Volume crystallization and microwave dielectric properties of indialite/cordierite glass by TiO_2 addition. *Ceram. Int.* **2021**, 47, 2735-2742. DOI: [10.1016/j.ceramint.2020.09.126](https://doi.org/10.1016/j.ceramint.2020.09.126)
- [7] Wang, F.; Lai, Y.; Zhang, Q.; Yang, X.; Li, B.; Wu, C.; Su, H.; Jiang, G.; Improved microwave dielectric properties of $(\text{Mg}_{0.5}\text{Ti}_{0.5})^{3+}$ Co-substituted $\text{Mg}_2\text{Al}_4\text{Si}_5\text{O}_{18}$ cordierite ceramics. *Solid State Sci.* **2022**, 132, 106989. DOI: [10.1016/j.solidstatesciences.2022.106989](https://doi.org/10.1016/j.solidstatesciences.2022.106989)
- [8] Lou, W.; Mao, M.; Song, K.; Xu, K.; Liu, B.; Li, W.; Yang, B.; Qi, Z.; Zhao, J.; Sun, S.; Lin, H.; Hu, Y.; Zhou, D.; Wang, D.; Reaney, I.M.; Low permittivity cordierite-based microwave dielectric ceramics for 5G/6G telecommunications. *J. Eur. Ceram. Soc.* **2022**, 42, 2820-2826. DOI: [10.1016/j.jeurceramsoc.2022.01.050](https://doi.org/10.1016/j.jeurceramsoc.2022.01.050)
- [9] Ebrahimi, F.; Nemati, A.; Banijamali, S.; Fabrication and microwave dielectric characterization of cordierite/BZBS ($\text{Bi}_2\text{O}_3\text{-ZnO-B}_2\text{O}_3\text{-SiO}_2$) glass composites for LTCC applications. *J. Alloys Compd.* **2021**, 882, 160722. DOI: [10.1016/j.jallcom.2021.160722](https://doi.org/10.1016/j.jallcom.2021.160722)
- [10] Wang, F.; Zhang, W.; Chen, X.; Mao, H.; Synthesis and characterization of low CTE value $\text{La}_2\text{O}_3\text{-B}_2\text{O}_3\text{-CaO-P}_2\text{O}_5$ glass/cordierite composites for LTCC application. *Ceram. Int.* **2019**, 45, 7203-7209. DOI: [10.1016/j.ceramint.2018.12.228](https://doi.org/10.1016/j.ceramint.2018.12.228)
- [11] Chen, G.H.; Sintering, crystallization and properties of CaO doped cordierite-based glass-ceramics. *J. Alloys Compd.* **2008**, 455, 298-302. DOI: [10.1016/j.jallcom.2007.01.036](https://doi.org/10.1016/j.jallcom.2007.01.036)
- [12] Mei, S.; Yang, J.; Ferreira, J.M.; Martins, R.; Optimization of parameters for aqueous tape-casting of cordierite-based glass ceramics by Taguchi method. *Mater. Sci. Eng. A.* **2002**, 334, 11-18. DOI: [10.1016/S0921-5093\(01\)01773-7](https://doi.org/10.1016/S0921-5093(01)01773-7)
- [13] Synkiewicz, B.; Szwagierczak, D.; Kulawik, J.; Multilayer LTCC structures based on glass-cordierite layers with different porosity. *Microelectron. Int.* **2017**, 34, 110-115. DOI: [10.1108/MI-12-2016-0084](https://doi.org/10.1108/MI-12-2016-0084)
- [14] Feng, K.C.; Chou, C.C.; Tsao, C.Y.; Chu, L.W.; Raevski, I.P.; Chen, H.; A novel phase-controlling-sintering route for improvement of diopside-based microwave dielectric materials. *Ceram. Inter.* **2015**, 41, 526-529. DOI: [10.1016/j.ceramint.2015.03.126](https://doi.org/10.1016/j.ceramint.2015.03.126)
- [15] Lai, Y.; Su, H.; Wang, G.; Tang, X.; Liang, X.; Huang, X.; Li, Y.; Zhang H., Ye, C.; Wang, X.R.; Improved microwave dielectric properties of $\text{CaMgSi}_2\text{O}_6$ ceramics through CuO doping. *J. Alloys Compd.* **2019**, 772, 40-48. DOI: [10.1016/j.jallcom.2018.09.059](https://doi.org/10.1016/j.jallcom.2018.09.059)

- [16] Huang, F.; Su, H.; Zhang, Q.; Wu, X.; Li, Y.; Tang, X.; Na-doped diopside microwave ceramics with dielectric properties influenced by the sintering, lattice vibration and chemical bond characteristics. *J. Alloys Compd.* **2022**, 896, 162973. DOI: [10.1016/j.jallcom.2021.162973](https://doi.org/10.1016/j.jallcom.2021.162973)
- [17] Huang, F.; Su, H.; Jing, Y.; Li, Y.; Lu, Q.; Tang, X.; Microwave dielectric properties of glass-free $\text{CaMg}_{0.9-x}\text{Li}_{0.2}\text{Zn}_x\text{Si}_2\text{O}_6$ ceramics for LTCC applications. *Ceram. Int.* **2020**, 46, 18308-18314. DOI: [10.1016/j.ceramint.2020.05.052](https://doi.org/10.1016/j.ceramint.2020.05.052)
- [18] Weng, Z.Z.; Song, C.X.; Xiong, Z.X.; Xue, H.; Sun, W.F.; Zhang, Y.; Yang, B.; Reece, M.J.; Yan, H.X.; Microstructure and broadband dielectric properties of Zn_2SiO_4 ceramics with nano-sized TiO_2 addition. *Ceram. Int.* **2019**, 45, 13251-13256. DOI: [10.1016/j.ceramint.2019.04.011](https://doi.org/10.1016/j.ceramint.2019.04.011)
- [19] Synkiewicz-Musialska, B.; Szwagierczak, D.; Kulawik, J.; Pałka, N.; Bajurko, P.R.; Impact of additives and processing on microstructure and dielectric properties of willemite ceramics for LTCC terahertz applications, *J. Eur. Ceram. Soc.* **2020**, 40, 362-370. DOI: [10.1016/j.jeurceramsoc.2019.10.005](https://doi.org/10.1016/j.jeurceramsoc.2019.10.005)
- [20] Kan, A.; Hirabayashi, R.; Takahashi, S.; Ogawa, H.; Low-temperature crystallization and microwave dielectric properties of forsterite generated in MgO-SiO_2 system following LiF addition. *Ceram. Int.* **2023**, 49, 9883-9892. DOI: [10.1016/j.ceramint.2022.11.163](https://doi.org/10.1016/j.ceramint.2022.11.163)
- [21] Zhou, J.; Towards rational design of low-temperature co-fired ceramic (LTCC) materials, *J. Adv. Ceram.* **2012**, 1, 89-99. DOI: [10.1007/s40145-012-0011-3](https://doi.org/10.1007/s40145-012-0011-3)
- [22] Ma, M.; Wang, Y.; Navarro-Cia, M.; Liu, F.; Zhang, F.; Liu, Z.; Li, Y.; Hanham, S.M.; Hao, Z.; The dielectric properties of some ceramic substrate materials at terahertz frequencies. *J. Eur. Ceram. Soc.* **2019**, 39, 4424-4428. DOI: [10.1016/j.jeurceramsoc.2019.06.01](https://doi.org/10.1016/j.jeurceramsoc.2019.06.01)

Copyright: © 2023 by the authors. Submitted for possible open access publication under the terms and conditions of the Creative Commons Attribution (CC BY) license (<https://creativecommons.org/licenses/by/4.0/>)

